Journal of Applied Polymer Science

Polycarbonate/1-(2-hydroxyethyl)-2,3-dimethylimidazolium chloride composite membranes and short-range chain mobility analysis

Lucas Mendonça da Rocha Oliveira, Priscila Vedovello, Caio Marcio Paranhos
Department of Chemistry, Federal University of São Carlos, São Carlos, São Paulo CEP 13565-905, Brazil
Correspondence to: L. M. da Rocha Oliveira (E-mail: l_lucasmro@yahoo.com.br)

ABSTRACT: In this investigation, the incorporation of imidazolium salt, 1-(2-hydroxehtyl)-2,3-dimethylimidazolium chloride [hydemmim][Cl] within bisphenol A polycarbonate (PC) matrix and the subsequent formation of membranes via casting were studied. Characterizations that aimed to establish structure-property correlations by Fourier transform infrared spectroscopy, differential scanning calorimetry, thermogravimetric analysis, dynamic mechanical thermal analysis, and water vapor transport (WVT) were performed. The results indicated that the presence of ionic liquid (IL) within the PC matrix significantly alter the local and macromolecular structure. The thermal stability is increased for all levels of incorporation. The plasticizing and antiplasticizing effects were observed due to the influence of the proportions of IL incorporated and of the cation's substituent chain of this IL. Distinct mechanisms of WVT were also observed in the presence of IL. © 2017 Wiley Periodicals, Inc. J. Appl. Polym. Sci. **2017**, *134*, 45117.

KEYWORDS: composites; ionic liquids; membranes; polycarbonates

Received 21 December 2016; accepted 16 March 2017
DOI: 10.1002/app.45117

INTRODUCTION

Ionic liquids (ILs) are a new class of solvents, receiving the classification of "green solvents" once their vapor pressures at room temperature are low. Therefore, these salts are liquid at room temperature.[1–3] They consist of inorganic anions arranged asymmetrically with organic cations.

The main characteristics of IL comprise low flammability, high thermal and chemical stability, high ionic conductivity, and potential to be used as solvent.[2–4] Among the IL are, for example, ammonium,[5,6] pyridinium,[7] phosphonium,[8–10] and imidazolium[11–14] salts. Imidazolium and its salts are one of the most studied ILs, like *N*-vinilimidazolinium,[15] 1-ethyl-3-methylimidazolium,[16] 1-butyl-3-methylimidazolium, and 1-octyl-3-methylimidazolium.[17] Awad *et al.*,[18] in 2004, studied thermal degradation of a series of alkyl-imidazolium salts and verified that the thermal stability of theses salts depends not only on the substituent group but also on the type of the anion.

They have application in electrochemistry,[19,20] catalysis,[21–23] nanotechnology,[6,18,24,25] and other areas.[26–28] In polymer science, ILs are widely used not only as solvents in polymerization processes[19,29] but also as components of the polymeric matrixes.[16,30] In the area of supported ILs, they are absorbed by imbibition or solubilization within polymeric matrix, like polymeric membranes, porous matrix, or bulk material.[2]

In polymeric membranes, authors conducted the ILs incorporation within Nafion membranes by immersion.[17,31] Yang *et al.*[31] immersed solutions of ILs by pre-established periods in Nafion membranes monitoring the incorporation levels by pH measures and conductivity of the solutions. Friess *et al.*[16] incorporated IL by stirring followed by solvent evaporation, relating the presence of IL with changes in the transport properties of gases, such as permeation and diffusion. Shindo *et al.*[32] prepared, by casting, composite membranes containing imidazolium salt and verified that the thermal stability and the selective CO_2/H_2 performance improved with the increase of IL content. It is also reported in the literature the obtaining of membranes based on ILs polymerization[15,33] and the preparation of liquid membranes.[34–37]

The unique properties of bisphenol A polycarbonate (PC) include optical transparency, high mechanical strength, thermal stability, toughness, and electrical properties.[38–40] These properties offer PC a large number of applications, as in electronics, optics, track etched membranes, and medical devices.[5,41–47] Smitha *et al.*[48] performed the sulfonation of some commercial aryl main chain polymers including the PC, and processed the membranes by casting. With the modification of PC these authors were able to find good properties, such as ion exchange capacity, tensile strength, and thermal stability. However, some recent articles can be found in literature about the modification of PC with IL, and not only with the modification of PC by covalent

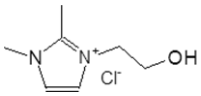

Figure 1. Molecular structure of 1–(2-hydroxyethyl)-2,3-methylimidazolium chloride [hydemmim][Cl].

groups linked. Rogalsky *et al.*[28] incorporated a series of imidazolium salts by casting and verified a reduction on thermal decomposition in comparison with neat PC. Xing *et al.*[5] incorporated ammonium salt in PC, hot-pressed the samples and then observed plasticization effect of the IL on PC and the better ductility.

Besides the number of papers devoted to IL-based polymeric membranes, the main scope is focused on specific properties such mechanical, thermal and transport properties. However, few investigations on the local (short-range) interactions between ILs and polymeric matrices were found. It is well known that short-range changes in macromolecules can alter the transport properties (diffusion, sorption, and permeation) in polymeric membranes. This knowledge can be applied to enhance the separation/selectivity characteristics of these membranes in several applications as nanoultrafiltration, gas separations, and polymer electrolyte membranes fuel cell. Thus, the present investigation may contribute to understanding the presence of IL within a vitreous polymeric matrix and its effects on local and macromolecular scale.

EXPERIMENTAL

Synthesis of 1–(2-Hydroxyethyl)-2,3-Dimethylimidazolium [Hydemmim][Cl] IL

For the synthesis of 1–(2-hydroxyethyl)-2,3-dimethylimidazolium [hydemmim][Cl] IL shown in Figure 1, the proposal reported by Tonle *et al.*[49] was used. Briefly, 2-cloroetanol (Merck) was added dropwise in 1,2-dimethylimidazoline (Sigma-Aldrich). First, the reaction mixture was stirred at room temperature for 20 min and then at 80 °C during 48 h under an inert nitrogen atmosphere. The excess of 1,2-dimethylimidazoline was extracted with ethyl ether.

Preparation of PC Membranes with Incorporation of IL

PC solutions (Lexan 101, GE Plastics) 10% (w/v) in dichloromethane (DCM) were prepared under mechanical stirring until complete dissolution of the polymer. Then, the IL was added in proportions of 1%, 5%, and 10% ($v/w_{polymer}$). The resulting solutions were kept under mechanical stirring for 12 h and brought to a IKA Turrax homogenizer during 2 min at 11,000 rpm.

The membranes were prepared by solvent evaporation method—casting. The solutions obtained were spread on glass plates with the aid of a doctor blade with 40 μm wet thickness, isolated from DCM saturated atmosphere, until the film formed and then dried in an oven during 12 h at 80 °C.

Measurements and Characterizations

The structure of the imidazolium salt was confirmed by NMR. The NMR spectra were obtained at ambient temperature on a Bruker Advance 400. ^{13}C-NMR measurements were performed at 100 MHz using D_2O as solvent. For ^{1}H-NMR measurements, the analysis was performed at 400 MHz, using $CDCl_3$ as solvent. The chemical shifts were reported relative to TMS internal standard.

Polymeric matrix and IL interactions were observed using a Fourier transform infrared spectroscopy (FTIR) Varian model 3100 with an attenuated total reflectance (ATR) accessory with resolution of 2 cm^{-1} and 20 scans at room temperature in the wavenumber range of 600 to 4000 cm^{-1}. The analysis of pure IL was used the transmittance mode.

The thermal stability of the membranes was evaluated by the decomposition initiation temperature, T_{onset}, by thermogravimetric analysis (TGA) on TA Instruments Q50 equipment under N_2 flow at a rate of 20 °C/min in the range of 30 to 800 °C.

The membranes were characterized in terms of their glass transition temperature (T_g) by differential scanning calorimetry (DSC) on TA Instruments Q2000 equipment under N_2 flow. Heating and cooling cycles were used at 20 to 180 °C at a rate of 20 °C/min. The T_g was determined in the second heating scan at the inflection point method.

The mechanical strength of the membranes was determined by analyzing the curve of storage elastic modulus (E') versus temperature on a thermodynamic and mechanical analyzer [dynamic mechanical thermal analysis (DMTA)] Q800, TA Instruments. Initially, the samples were cooled and kept isothermally at −120 °C during 3 min. Then the samples were submitted to heating 3 °C/min in a vibrational frequency of 10 Hz to 160 °C. The deformation amplitude of 25 μm was kept in order to maintain the linear viscoelastic profile.

The water vapor transport (WVT) was done to establish the relation between the mobility of the polymeric chains and the water vapor affinity, and considering that the transport mechanism is given by sorption-diffusion type. WVT measures were performed in accordance with ASTM E 96 at 30 °C. Glass-based Payne permeability cups were filled with deionized water and sealed with the prepared membranes with diameter equal to that of glass. These cups were then brought to a desiccator containing a glass dish filled with phosphorus pentoxide (P_2O_5) to ensure that the environment does not saturate with water vapor ($a_w = 0$). Inside of the Payne cups, the activity of the penetrating is equal to 1 ($a_w = 1$), referring to deionized water. The Payne cups were weighed and verified for water loss for 17 days. From the linear regression of the experimental points, WVT value was determined by the ratio of the weight variation corrected by the membrane exposed area and using Fick's first law, which is the ratio between the flow field and the concentration gradient [eq. (1)]:

$$\mathrm{WVT} = \frac{\Delta m}{\Delta t\ A_d}\left(\frac{\mathrm{g}}{\mathrm{day\ m^2}}\right) \quad (1)$$

where $\frac{\Delta m}{\Delta t}$ = slope of the curve, A_d = area of the film

RESULTS AND DISCUSSION

Nuclear Magnetic Resonance

The NMR characterization proved the synthesis of IL. The NMR ^{13}C shifts obtained were 34.1 ($\mathbf{C}H_3$—N); 46.8 (HO—CH_2—$\mathbf{C}H_2$—N);

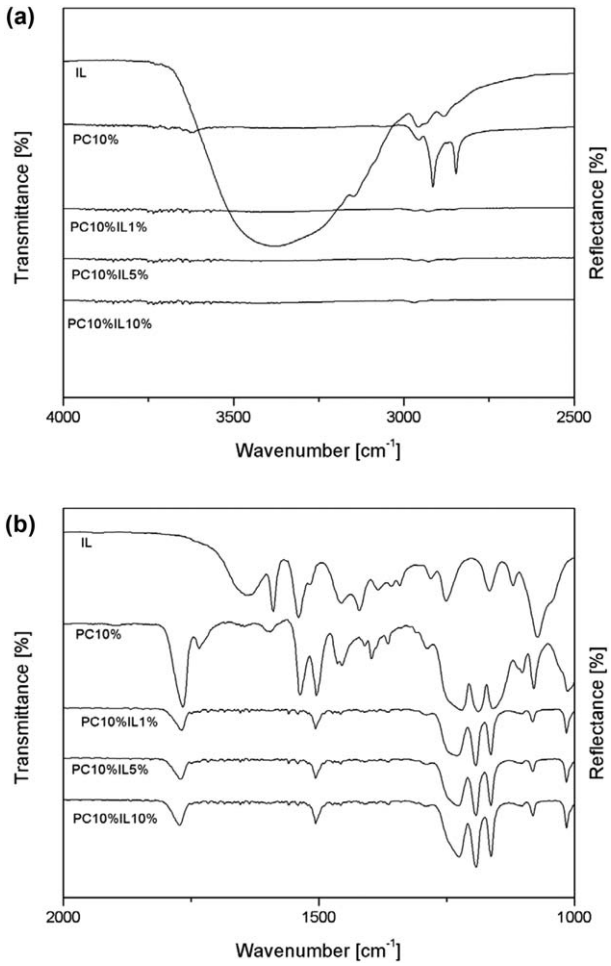

Figure 2. (a) FTIR-ATR spectra between 4000 and 2500 cm^{-1}. (b) FTIR-ATR spectra between 2000 and 1000 cm^{-1}.

121.5 (imidazoline ring **C**—**C**—N); and 142.0 (imidazole ring N—**C**—N) ppm, and for the NMR ^1H spectrum, shifts were observed shifts in 3.84 (m, 3 H, C**H**$_3$-N); 3.86 (m, 2 H, HO-CH_2-C**H**$_2$-N); 4.27 (m, 2 H, HO-C**H**$_2$-CH_2-N); 7.45-7.5 (m, 2 H, imidazoline ring) ppm according to the literature reported.[49,50]

Infrared Spectroscopy

Through the prepared membranes and their precursors FTIR spectra was able to verify some changes in active bands, indicating interactions between the IL and PC (Figure 1). The main PC active bands found were in 1230, 1175, 1153 cm^{-1} (C—O stretching motion); 1465, 1390 cm^{-1} (CH_3 deformation vibration); 1073 cm^{-1} (C—H deformation vibration of phenyl ring hydrogens); 1500 cm^{-1} (C—C stretching vibration of phenyl); 1770 cm^{-1} (free carbonyl stretching motion); and 2970, 2850 cm^{-1} (CH_3 stretching vibration).[47,51]

In IL FTIR spectrum, it was possible to see a wide and intense band in the region of 3100 to 3500 cm^{-1} [Figure 2(a)] related to vibration of hydroxyl groups, possibly due to water contained in the material and also to the vibration of the terminal hydroxyl substituent chain of the organic salt. This peak is also observed by other authors that synthetized IL with hydroxyl terminal groups.[24,52] Active bands in the FTIR regarding the imidazoline ring have been reported by some authors in their respective studies on ILs, and a close agreement between the vibrations related to the imidazoline ring exists in 2949 cm^{-1} (C—H stretching in methyl group); 1535 to 1471 cm^{-1} (C=C and C=N stretching within the imidazoline ring and C—H bending-in-plane); 1159 cm^{-1} (C=N stretching) and 858 and 751 cm^{-1} (C—H bending-out-of-plane).[11,52]

Referring to the ATR FTIR spectrum obtained from the membranes modified with IL, it is possible to verify the absence of the hydroxyl band [Figure 2(b)]. It is believed that an "imprisonment" of hydroxyl groups occurs, precluding active modes in infrared. The absence of the signal may be related to interactions of hydrogen bonding type between the terminal hydroxyl group of IL and the carbonyl of the carbonate group of the PC chain. The region of the asymmetric stretches of methyl groups of PC around 2970 cm^{-1} was not checked on IL/PC composite indicating that, locally, molecules of IL may be making difficult the vibrations that result in these signs.

TGA

A higher thermal stability was observed on all the cases in which IL incorporated the membranes. The highest value of T_{onset} is seen at 5% of IL (Table I). The compilation of all TGA curves [Figure 3(a)] shows that the membrane of PC degrades in one step. The degradation process takes place between 410 and 600 °C with maximum degradation temperature at around 521 °C.[38,40] The process occurs in multiple steps to IL, better visualized by the DTGA curve in Figure 3(b). The first step at 100 °C, referring to water loss, the second at around 205 °C, due to the beginning of hydroxyethyl decomposition, the IL group substituent. The second stage, more evident than the others, has T_{onset} at 302 °C and a maximum peak at around 346 °C related to degradation imidazolium ring. By DTGA, it is possible to see that the membranes with IL showed subtle peaks at around 260 °C, a different value comparing to the IL degradation. This demonstrates that the degradation process takes place through different mechanisms with the incorporation of the organic salt, due to the interactions between the matrix and IL.

DSC

Figure 4 compiles the results obtained by DSC. Pure polycarbonate membrane showed high T_g at 150.0 °C,[48] justified by the value of stiffness of the polymeric chains, thanks to the presence of aromatic rings that restrict the mobility of these chains. Table II gives the T_g values for the series of IL-PC membranes. For membranes modified with 1% of IL, there was a decrease in T_g,

Table I. Onset Degradation Temperature Values and Maximum Degradation Temperature Found by TGA

Sample	T_{onset} (°C)	T_{max} (°C)
IL	302.24	346.58
PC 10%	467.04	520.41
PC 10% IL 1%	469.06	519.12
PC 10% IL 5%	495.60	536.00
PC 10% IL 10%	481.89	529.88

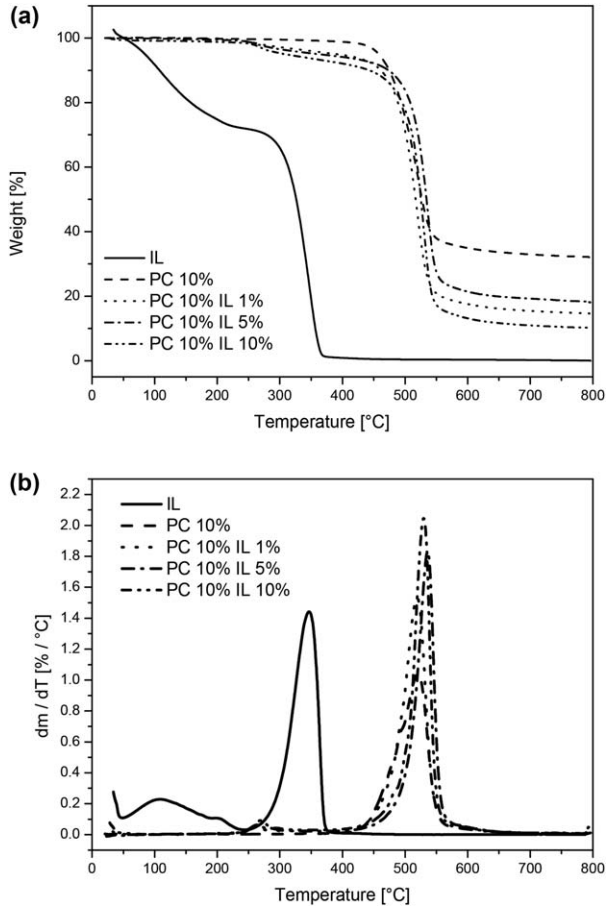

Figure 3. (a) TGA curves of IL and all the modified membranes. (b) DTGA curves of IL and all the modified membranes.

indicating a possible beginning of the polymer plasticization process. However, for modification with 5% the T_g value kept constant without changes on macromolecular level. With the modification of 10%, a significant reduction in T_g would show a more significant process of plasticization, but this result could not be justified by the creation of voids due to the incorporation of IL at macromolecular level. The result obtained by DMTA, that will be seen later, showed an increase in storage modulus, indicating an antiplaticization phenomenon.

Dynamic Mechanical Thermal Analysis

Table II also shows the results obtained by DMTA. The values of storage moduli (E') [Figure 5(a)] were taken for the ambient temperature at 25 °C. It is possible to see that the behavior is nonlinear, since there was neither a decrease nor an increase in the E' according to the percentage of IL incorporated. For the concentration of 1% IL, there was a significant decrease in the E' value, that is, a significant lower mechanical strength in the material, indicating a plasticization effect, which corroborates the T_g temperature by DSC and also by DMTA. For 5% of IL incorporated, an increase in the value of E' was observed and thus a macromolecular antiplasticization effect may be related. The increase in E' confirms the increase of the T_g value comparing with pure matrix PC. However, in the case of 10% of IL incorporated, there was an increase in E' followed by a decrease in T_g temperature. Therefore, for a better understanding of the system, the loss modulus E'' versus temperature curve [Figure 5(b)] was analyzed.

The curve for the membrane of 10% PC shows that the T_g at around 153 °C is in agreement with the value found by DSC. The presence of three others subtransitions can also be verified. At around −102 °C there is a transition that is quite characteristic of the PC, phenyl ring π-flips,[53] which refers to PC conformation changes, involving bond rotations of two neighboring carbonate groups, changing the conformation from *trans-cis* to *trans-trans*.[54] Such movement requires rotation around the CO bond with an inversion of the phenyl groups leading to fluctuations in the free volume as a result of bisphenol A translation. Others peaks observed at around the 0 and 30 °C for PC refer to a relaxation of tension in the membranes preparation, and this strain may be caused by the inner orientation of side groups or defects that occur during the packaging in the vitreous state.

There is a decrease in the value of T_g for the 1% of IL incorporation compared to pure matrix as well as in the DSC and therefore a long range molecular motion involving segments of the chain occurs. The decrease in the E', as previously mentioned, consolidates the plasticizing and, through a local analysis, it is possible to verify peak shifts of relaxation subtransitions related to PC. There was an increase in β–T_g, −94 °C, indicating that the presence of IL in regions of ring-flip motions of PC make this conformational change difficult.

The 5% of incorporation showed an increase in both the T_g and E' values, indicating an antiplasticizing effect. The β-T_g increases at around 20 and 10 °C compared to the neat matrix and to 1% of IL, respectively, showing that a higher energy level is required to drive the ring-flip local motion in the highest concentration of IL. This result reveals that plasticizers can offer the opposite behavior, that is, plasticizers can suppress the secondary transition, leading to an antiplasticization process by mechanisms in which the plasticizers may occupy the free volume in the polymer restricting the molecular movements that are responsible for the sub-T_g transitions.[55] Figure 6(a) represents in a simple manner the presence of IL molecules occupying regions that hindering the β-T_g.

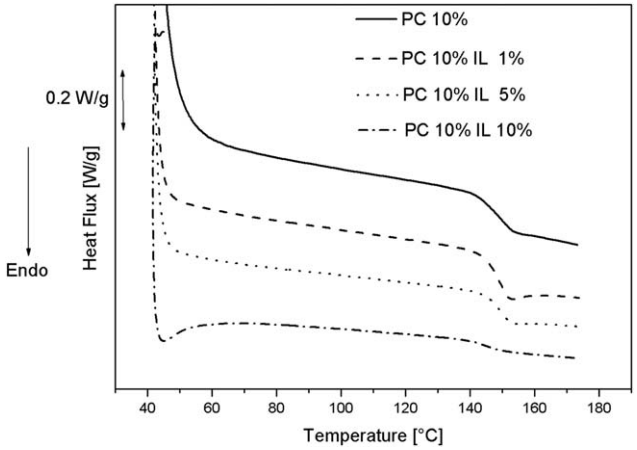

Figure 4. DSC curves of the modified membranes with IL.

Table II. Compilation of the Results of WVT, T_g, β–T_g, and E' for the Understanding of the Mechanism by Which the Transport of Water Vapor Occurs

Sample	WVT (g/d m^2)	T_g (°C) DSC	T_g (°C) DMTA	β–T_g (°C)	E' (MPa)
PC 10%	41.1	150.0	153.02	−102.62	2244
IL 1%	115.0	148.8	151.61	−93.92	1675
IL 5%	81.0	150.3	154.72	−81.49	2348
IL 10%	137.0	145.0	146.64	−111.32	2315

Referring to the results obtained by FTIR-ATR, the characteristic peaks of asymmetric stretching of methyl groups cannot be seen at around 2970 cm^{-1} with the incorporation of IL for all concentrations, so it is possible to establish that this region is also occupied by the organic salt [Figure 6(b)].

At 10% a lower T_g value is found, followed by an increase in the E' value. This mobility at long range, reinforced with stiffening of the vitreous phase, is a characteristic of an antiplasticized system. The antiplasticization produces a reduction in free volume and also in T_g of the glassy polymer.

In this case, there is a local plasticizing effect below the T_g. β–T_g at around −110 °C reveals a reduction of the energy required to local movement. Another subtransition, γ-T_g, is seen at around 50 °C, also characterized by the ring-flip motion but with a more difficult movement. The content of IL is sufficient for the formation of clusters of the liquid itself, where interactions among IL molecules happen. This originates regions that are less exposed to deformation than others, due the presence of small clusters. Therefore, the signal supplied is given by the ring-flip movement under the influence of these clusters [Figure 6(c)].

Performing a direct comparison between the content of IL incorporated and the values of β–T_g (Figure 7), it is possible to verify that for 1% and 5% a local antiplasticization effect takes place, with an increase in the value of the sub-T_g, with maximum value found at 5%. The antiplasticization effect, is justified by the interactions of hydrogen bonding between the terminal hydroxyl substituent chain of the IL and the CO group of the PC. On the other hand, a local plasticizing effect is seen at 10% of IL incorporated. As mentioned before, at the

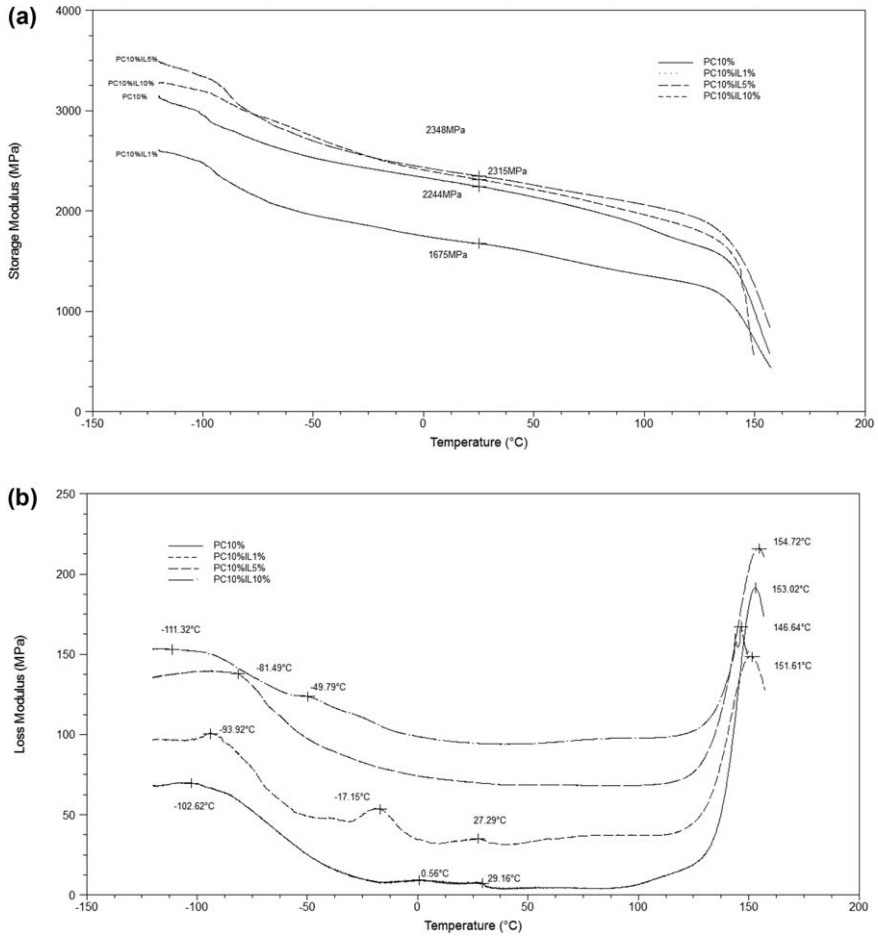

Figure 5. (a) Storage modulus versus temperature curves for IL-PC membranes. (b) Loss modulus versus temperature curves for IL-PC membranes.

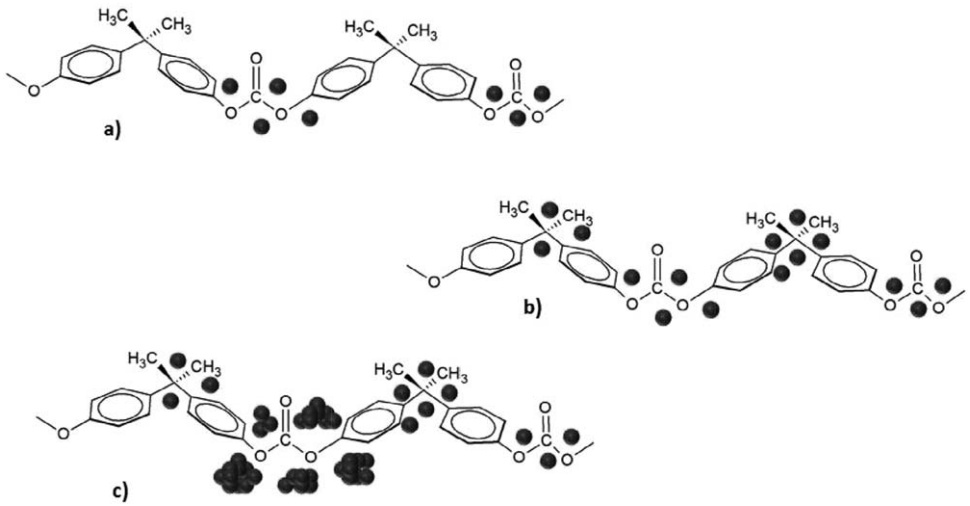

Figure 6. (a) PC under the influence of IL on the rotation of carbonate group, (b) dispersion of IL at the local level, and (c) IL clustering in regions of the polymer chain.

concentrations of 1% and 5% great dispersion happened, with IL molecules occupying local voids of the polymer chains to the point of hindering the movement of this sub transition. The content of 10% reveals high concentration of IL, in which the movement is then given by the PC segment phenyl-carbonate-phenyl on the influence of IL clusters.

WVT

Table II gives the values found by WVT analysis of modified samples with IL. With this modification, a significant increase can be seen in WVT values comparing to the PC matrix showing the possibility of paths that favor the transport of water vapor through the membrane. One possibility that favors the permeation on local and macromolecular levels are voids, while another possibility is the formation of IL clusters which can create preferential paths for the permeation of water vapor.

The values found in WVT and the values of glass transition temperature were compiled in the same graph as shown below (Figure 8). The graph shows that a decrease in the T_g leads to an increase in the WVT, because the reduction of T_g leads to an increase in chain mobility, facilitating the transport of water vapor. The hydrophobic character of PC is decreased by the incorporation of IL, which also justifies the increase in WVT. The presence of the hydroxyl terminal group of the substituent on the imidazole ring is favorable to affinity with water vapor.

The compilation done on Table II represents a study of T_g and β–T_g in WVT values.

A decrease in the alpha transition, corroborating the decrease in the storage modulus, shows that the incorporation of IL generated voids at macromolecular scale, justifying the WVT values observed at 1% incorporation. The subtransition temperature rose and then more difficulties appeared in the characteristic movements of such transition. Therefore, the highest value of WVT found is given by the preferential permeation through voids at macromolecular scale, as shown in region (b) of Figure 9.

With the incorporation of 5%, the WVT increased compared to pure PC. The membrane had a similar T_g value compared to not incorporated membranes and an increase in E', revealing a higher mechanical strength. However, at the local level there was an increase in β–T_g which hinders the relaxation. Thus if there was neither local favoring for the permeation of water vapor nor major changes at macromolecular level, it is believed, that in this case, the main responsible factor for the WVT

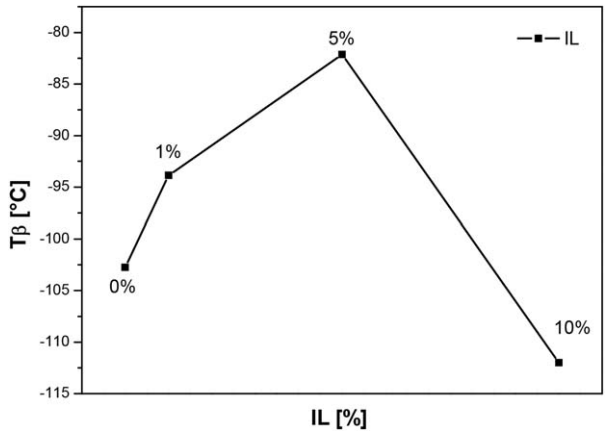

Figure 7. Relation between β-T_g and level of IL incorporated in PC membranes.

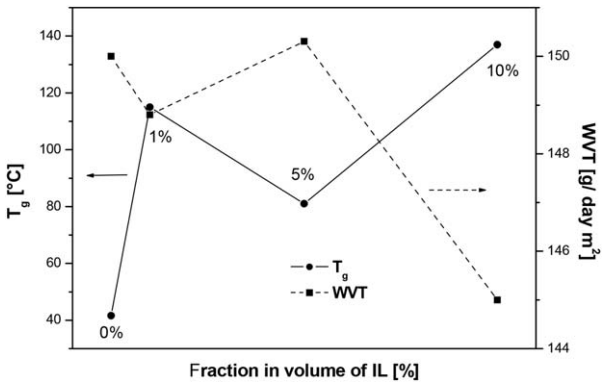

Figure 8. Relation between T_g and WVT in IL-PC membranes.

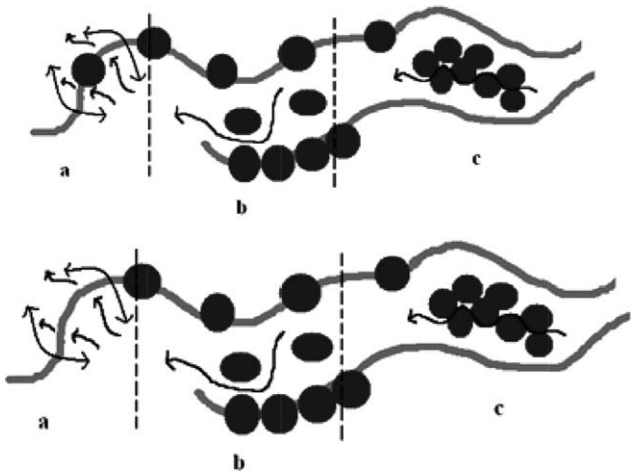

Figure 9. (a) Representation of the local movement responsible for β transition, under influence of IL or not; (b) representation of the macromolecular mobility, responsible for the T_g decrease created by voids origined by IL incorporation and (c) preferred paths given by IL.

increase is the IL, which is created pathways that favor this process, as represented by the region (c) of Figure 9.

At the incorporation of 10%, a considerable increase in WVT, a reduction in T_g, an increase of E' occurred, which, as previously mentioned, is an antiplasticized system, where the reduction in the free volume at macromolecular level and the T_g decrease happened. β–T_g decreased, so the transition was facilitated. It can be inferred that the locally plasticized system and the preferred paths given by IL, considerably increased the value of WVT, as represented by the region (a) and (c) of the Figure 9.

CONCLUSIONS

The IL acts at macromolecular and local scale on PC, as evidenced by spectroscopic and thermal characterizations. The membranes modified with 5% of IL appear to be more thermal resistant, with higher onset degradation temperature. Different mechanisms of water vapor permeation occur depending on the content of IL incorporated. The permeation process was observed by three different forms, it can happen at macromolecular level, with the movement of longer segments of the polymer chains due to the voids presence, it can also happen locally due to the presence of local voids that gives mobility to shorter segments of the polymer chains and, at last, the WVT permeation can be assisted by IL clusters due to their hydrophilic character.

ACKNOWLEDGMENTS

The authors thank CNPQ (Conselho Nacional do Desenvolvimento Científico e Tecnologico) for research grants.

REFERENCES

1. Mercerreyes, D. *Prog. Polym. Sci.* **2011**, *36*, 1629.
2. Lu, J. M.; Yan, F.; Texter, J. *Prog. Polym. Sci.* **2009**, *34*, 431.
3. Keskin, S.; Kayrak-Talay, D.; Akman, U.; Hortaçsu, Ö. *J. Supercrit. Fluids* **2007**, *43*, 150.
4. Wu, W.; Li, W.; Han, B.; Zhang, Z.; Jiang, T.; Liu, Z. *Green Chem.* **2005**, *7*, 701.
5. Xing, C.; Zheng, X.; Xu, L.; Jia, J.; Ren, J.; Li, Y. *Ind. Eng. Chem. Res.* **2014**, *53*, 4304.
6. Kim, S.; Park, S. *J. Colloid Interface Sci.* **2009**, *332*, 145.
7. Calvar, N.; Gómez, E.; Macedo, E. A.; Domínguez, Á. *Thermochim. Acta* **2013**, *565*, 178.
8. Livi, S.; Duchet-Rumeau, J.; Pham, T.; Gérard, J. *J. Colloid Interface Sci.* **2010**, *349*, 424.
9. Lall-Ramnarine, S. I.; Mukhlall, J. A.; Wishart, J. F.; Engel, R. R.; Romeo, A. R.; Gohdo, M.; Ramati, S.; Berman, M.; Suarez, S. N. *Beilstein J. Org. Chem.* **2014**, *10*, 271.
10. Tsunashima, K.; Sugiya, M. *Electrochem. Commun.* **2007**, *9*, 2353.
11. Chowdhury, A.; Thynell, S. T. *Thermochim. Acta* **2006**, *443*, 159.
12. Rao, G. R.; Rajkumar, T.; Varghese, B. *Solid State Sci.* **2009**, *11*, 36.
13. Patachia, S.; Friedrich, C.; Florea, C.; Croitoru, C. *eXPRESS Polym. Lett.* **2011**, *5*, 197.
14. Heimer, N. E.; Del Sesto, R.; Meng, Z.; Wilkes, J. S.; Carper, W. R. *J. Mol. Liq.* **2006**, *124*, 84.
15. Carlisle, T. K.; Nicodemus, G. D.; Gina, D. L.; Noble, R. D. *J. Membr. Sci.* **2012**, *397*, 24.
16. Friess, K.; Jansen, J. C.; Bazzarelli, F.; Izák, P.; Jarmarová, V.; Karcírková, M.; Schauer, J.; Clarizia, G.; Bernardo, P. *J. Membr. Sci.* **2012**, *415*, 801.
17. Neves, L. A.; Benavente, J.; Coelhoso, I. M.; Crespo, J. G. *J. Membr. Sci.* **2010**, *347*, 42.
18. Awad, W. H.; Gilman, J. W.; Nyden, M.; Harris, R. H.; Sutto, T. E.; Callahan, J.; Truvole, P. C.; DeLong, H. C.; Fox, D. M. *Thermochim. Acta* **2004**, *409*, 3.
19. Al Zoubi, M.; Endres, F. *Electrochim. Acta* **2011**, *56*, 5872.
20. El Abedin, S. Z.; Endres, F. *Electrochim. Acta* **2009**, *54*, 5673.
21. Li, L.; Liu, F.; Li, Z.; Song, X.; Yu, S.; Liu, S. *Fiber Polym.* **2013**, *14*, 365.
22. Welton, T. *Coord. Chem. Rev.* **2004**, *248*, 2459.
23. Olivier-Bourbigou, H.; Magna, L.; Morvan, M. D. *App. Catal. A* **2010**, *373*, 1.
24. Goswami, S. K.; Ghosh, S.; Mathias, L. J. *J. Colloid Interface Sci.* **2012**, *368*, 366.
25. Steinhauser, D.; Subramaniam, K.; Das, A.; Heinrich, G.; Klüppel, M. *Express Polym. Lett.* **2012**, *6*, 927.
26. Sharma, P.; Choi, S.; Park, S.; Baek, I.; Lee, G. *Chem. Eng. J.* **2012**, *181*, 834.
27. El Seoud, O. A.; Koschella, A.; Fidale, L. C.; Dorn, S.; Heinze, T. *Biomacromolecules* **2007**, *8*, 2629.
28. Rogalsky, S.; Fatyeyeva, K.; Lyoshina, L.; Tarasyuk, O.; Bulko, O.; Lobok, S. *J. Appl. Polym. Sci.* **2004**, *131*, DOI: 10.1002/app.40050.
29. Kubisa, P. *Prog. Polym. Sci.* **2004**, *29*, 3.

30. Nancarrow, P.; Liang, L.; Gan, Q. *J. Membr. Sci.* **2014**, *472*, 222.
31. Yang, J.; Che, Q.; Zhou, L.; He, R.; Savinell, R. *Electrochim. Acta* **2011**, *56*, 5940.
32. Shindo, R.; Kishida, M.; Sawa, H.; Kidesaki, T.; Sato, S.; Kanehashi, S.; Nagai, K. *J. Membr. Sci.* **2014**, *454*, 330.
33. Yang, J.; Li, Q.; Jensen, J. O.; Pan, C.; Cleeman, L. N.; Bjerrum, N. J.; He, R. *J. Power Sources* **2012**, *205*, 114.
34. Lozano, L. J.; Godínez, C.; de los Ríos, A. P.; Hernández-Fernández, F. J.; Sánchez-Segado, S.; Alguacil, F. J. *J. Membr. Sci.* **2011**, *376*, 1.
35. Vangeli, O. C.; Romanos, G. E.; Beltsios, K. G.; Fokas, D.; Athanasekou, C. P.; Kanellopoulos, N. K. *J. Membr. Sci.* **2010**, *365*, 366.
36. Fortunato, R.; Afonso, C. A. M.; Reis, M. A. M.; Crespo, J. G. *J. Membr. Sci.* **2004**, *242*, 179.
37. de los Ríos, A. P.; Hernández-Fernández, F. J.; Tomás-Alonso, F.; Palacios, J. M.; Víllora, G. *Desalination* **2009**, *245*, 776.
38. Jang, B. N.; Wilkie, C. A. *Polym. Degrad. Stab.* **2004**, *86*, 419.
39. Liao, C.; Wang, C.; Shih, K.; Chen, C. *Eur. Polym. J.* **2011**, *47*, 911.
40. Feng, J.; Hao, J.; Du, J.; Yang, R. *Polym. Degrad. Stab.* **2012**, *97*, 605.
41. Diepens, M.; Gijsman, P. *Polym. Degrad. Stab.* **2007**, *92*, 397.
42. Hareesh, K.; Pandey, A. K.; Sangappa, Y.; Bhat, R.; Venkataraman, A.; Sanjeev, G. *Nucl. Instrum. Methods Phys. Res. Sect. B* **2013**, *295*, 61.
43. Sertova, N.; Balazant, E.; Toulemonde, M.; Trautmann, C. *Nucl. Instrum. Methods Phys. Res. Sect. B* **2009**, *267*, 1039.
44. Koivula, R.; Makkonen-Craig, M.; Harjula, R.; Paronen, M. *React. Funct. Polym.* **2012**, *72*, 92.
45. Cornelius, T. W.; Apel, P. Y.; Schiedt, B.; Trautmann, C.; Toimil-Molares, M. E.; Karim, S.; Neumann, R. *Nucl. Instrum. Methods Phys. Res. Sect. B* **2007**, *265*, 553.
46. Lue, S. J.; Lo, P. W.; Hung, L.; Tung, Y. L. *J. Power Sources* **2010**, *195*, 7677.
47. Feng, Y.; Wang, B.; Wang, F.; Zhao, Y.; Liu, C.; Chen, J.; Shen, C. *Polym. Degrad. Stab.* **2014**, *107*, 129.
48. Smitha, B.; Sridhar, S.; Khan, A. A. *J. Membr. Sci.* **2003**, *225*, 63.
49. Tonle, I. K.; Letaief, S.; Ngameni, E.; Detellier, C. *J. Mater. Chem.* **2009**, *19*, 5996.
50. Jalili, A. H.; Mehdizadeh, A.; Shokouhi, M.; Sakheinia, H.; Taghikhani, V. *J. Chem. Thermodyn.* **2010**, *42*, 787.
51. Kraus, R. G.; Emmons, E. D.; Thompson, J. S.; Covington, A. M. *J. Polym. Sci. Part B: Polym. Phys.* **2008**, *46*, 734.
52. Hossain, M. I.; El-Harbawi, M.; Alitheen, N. B. M.; Noaman, Y. A.; Lévêque, J.; Yin, C. *Ecotox. Environ. Safe.* **2013**, *87*, 65.
53. Whitney, D. R.; Yaris, R. *Macromolecules* **1997**, *30*, 1741.S0024-9297(96)01143-6
54. Cassu, S. N.; Felisberti, M. I. *Quím. Nova* **2005**, *28*, 255.
55. Larocca, N. M.; Pessan, L. A. *J. Membr. Sci.* **2003**, *218*, 69.